Proc. Natl. Acad. Sci. USA
Vol. 90, pp. 7523–7527, August 1993
Biochemistry

Crystal structures of medium-chain acyl-CoA dehydrogenase from pig liver mitochondria with and without substrate

(x-ray crystallography/flavoprotein/active site/fatty acid oxidation)

JUNG-JA P. KIM*, MING WANG, AND ROSEMARY PASCHKE

Department of Biochemistry, Medical College of Wisconsin, Milwaukee, WI 53226

Communicated by Helmut Beinert, April 5, 1993

ABSTRACT **The three-dimensional structure of medium-chain acyl-CoA dehydrogenase from pig mitochondria in the native form and that of a complex of the enzyme and a substrate (product) have been solved and refined by x-ray crystallographic methods at 2.4-Å resolution to *R* factors of 0.172 and 0.173, respectively. The overall polypeptide folding and the quaternary structure of the tetramer are essentially unchanged upon binding of the ligand, octanoyl (octenoyl)-CoA. The ligand binds to the enzyme at the rectus (re) face of the FAD in the crevice between the two α-helix domains and the β-sheet domain of the enzyme. The fatty acyl chain of the thioester substrate is buried inside of the polypeptide and the 3′-AMP moiety is close to the surface of the tetrameric enzyme molecule. The alkyl chain displaces the tightly bound water molecules found in the native enzyme and the carbonyl oxygen of the thioester interacts with the ribityl 2′-hydroxyl group of the FAD and the main-chain carbonyl oxygen of Glu-376. The C_α—C_β of the fatty acyl moiety lies between the flavin and the γ-carboxylate of Glu-376, supporting the role of Glu-376 as the base that abstracts the α proton in the α–β dehydrogenation reaction catalyzed by the enzyme. Trp-166 and Met-165 are located at the sinister (si) side of the flavin ring at the surface of the enzyme, suggesting that they might be involved in the interactions with electron transferring flavoprotein. Lys-304, the prevalent mutation site found in patients with medium-chain acyl-CoA dehydrogenase deficiency, is located ≈20 Å away from the active site of the enzyme.**

Mammalian acyl-CoA dehydrogenases [acyl-CoA:(acceptor) 2,3-oxidoreductase; EC 1.3.99.3] catalyze the first step in each cycle of fatty acid β-oxidation in mitochondria (1). Acyl-CoA thioesters are oxidized to the corresponding *trans*-2,3-enoyl-CoA products with concomitant reduction of enzyme-bound FAD. Reoxidation of the dehydrogenase flavin and the transfer of reducing equivalents to the mitochondrial respiratory chain are catalyzed by the soluble electron transferring flavoprotein (ETF) and the particulate ETF-ubiquinone oxidoreductase, an iron–sulfur flavoprotein (2, 3). Three soluble straight-chain acyl-CoA dehydrogenases have been isolated and classified according to their distinct but overlapping substrate specificities for long-, medium-, and short-chain fatty acids (4). Recently, a very-long-chain acyl-CoA dehydrogenase has been identified in the inner membrane of rat mitochondria (5). In addition, three dehydrogenases involved in amino acid metabolism, isovaleryl- (6), 2-methyl branched chain (7), and glutaryl- (8) CoA dehydrogenases, have been isolated and characterized. With the exception of the membrane-associated very-long-chain acyl-CoA dehydrogenase, these enzymes appear very similar in their catalytic mechanism and their biochemical properties. They are homotetramers and each subunit contains ≈400 aa residues and one equivalent of FAD. Medium-chain acyl-CoA dehydrogenase (MCAD) exhibits a broad chain-length specificity and has its highest activity with C_8-CoA. Recently, several genetic diseases have been found to be due to acyl-CoA dehydrogenase deficiencies. Deficiency of MCAD appears to be the most common among disorders of fatty acid oxidation in humans (9). It is manifested by fasting intolerance, hypoglycemic coma, failure of ketogenesis, dicarboxylic acidemia, and sudden infant death (10). Although the enzyme structure described in this report is that of the porcine liver enzyme, the amino acid sequence is very similar to that of the human enzyme (11), from which it differs by <10% conservative substitutions (A. W. Strauss, personal communication). Therefore, it is expected that structural conclusions drawn from the pig enzyme will apply to the human enzyme. We have reported the crystal structure of pig-liver MCAD at 3.0-Å resolution (12) and preliminary data on complexes of the enzyme and substrates (13). In this paper, we present the crystal structure of MCAD in the native form and that of a complex of the enzyme and the octanoyl-CoA, both refined at 2.4-Å resolution.† Comparison of these two structures allows us to locate the active site, to determine the interactions between the substrate and the polypeptide, and to make conclusions regarding the catalytic mechanism of the enzyme.

EXPERIMENTAL PROCEDURES

Crystallization. Enzyme purification and crystallization of the native enzyme crystals were carried out using the sitting-drop methods as described (12). The conditions for growing the crystals of the complex were similar to those for growing the native MCAD crystals except that the solution contained octanoyl-CoA equimolar with the active sites and the crystallization set-up procedures were performed in a glove box purged with nitrogen. The crystallization plates were tightly sealed with vacuum grease and were stored outside of the glove box at 4°C. Subsequent manipulations of the crystals of the complex were carried out anaerobically in the glove box. The crystals are isomorphous to the native crystals (Table 1). They are orthorhombic, space group $C222_1$, and contain two monomers per asymmetric unit.

Data Collection and Structure Determination. The diffraction data sets for the native and the complex crystals were collected to 2.4 Å at 4°C, using one single crystal each, with the Multiwire Area Detector System at the University of California-San Diego. The crystal structure of the native form was initially determined at 3.0-Å resolution by the multiple isomorphous replacement method, and the first model was

The publication costs of this article were defrayed in part by page charge payment. This article must therefore be hereby marked "*advertisement*" in accordance with 18 U.S.C. §1734 solely to indicate this fact.

Abbreviations: ETF, electron transferring flavoprotein; MCAD, medium-chain acyl-CoA dehydrogenase.

*To whom reprint requests should be addressed.

†The atomic coordinates have been deposited in the Protein Data Bank, Chemistry Department, Brookhaven National Laboratory, Upton, NY 11973 (references 1MDD and 1MDE).

Table 1. Data collection and refinement statistics

Parameter	Enzyme	
	Native	Complex
Unit-cell dimensions (a, b, c), Å	128.82, 136.144, 106.13	128.78, 137.25, 105.32
Total no. of observations	138,867	124,642
No. of unique reflections	30,930	36,088
Completeness of data at 2.4 Å, %	84	98
*R*sym*	0.047	0.072
Final crystallographic *R* factor	0.172	0.173
Total no. of nonhydrogen atoms (excluding H_2O molecules)	6070	6184
No. of H_2O molecules included	194	198
Average temperature factor, $Å^2$ (all atoms)	17.18	17.77
rms bond deviation from ideal, Å	0.008	0.009
rms angle deviation from ideal, degrees	1.2	1.3

*$R\text{sym} = \Sigma|I - \langle I\rangle|/\Sigma\langle I\rangle$ summed over all observations of all reflections.

built into an electron density map averaged about the noncrystallographic twofold axis (12). This model was adjusted to electron densities of appropriate difference Fourier maps with the aid of interactive graphics by using the program TOM/FRODO (14) to produce a starting model for the subsequent refinements. The standard crystallographic *R* factor for the data between 10.0-Å and 3.0-Å resolution was 0.36. Six rounds of simulated annealing refinements to 2.4-Å resolution by using the program X-PLOR (15), with manual adjustments between rounds, reduced the *R* factor to 0.275 for all data between 8.0-Å and 2.4-Å resolution. At this stage, the model was manually readjusted using omit maps and the subsequent refinements were performed by the restrained least-squares methods, using a modified version of PROLSQ (16). The final crystallographic *R* factor for all observed data in the resolution range from 8.0 Å to 2.4 Å was 17.2% including 194 water molecules. The structure of the complex was solved by the difference Fourier method. Difference Fourier maps with phase angles from the refined native protein structure, excluding the water molecules, were calculated and averaged about the noncrystallographic twofold axis (17). The initial model of the complexed structure obtained from the averaged electron density map gave an *R* factor 26.4% and was further refined by both simulated annealing and restrained least-squares methods with manual adjustments. The final model yielded an *R* factor of 17.3% including 198 water molecules. The data collection and refinement statistics for both the native and the complexed structures are given in Table 1. The amino acid sequence numbering used in this report refers to the mature human protein sequence (11).

RESULTS AND DISCUSSION

Initially, the sitting drop containing the enzyme–substrate complex for crystallization was colorless. However, after a couple of weeks, pale yellow crystals started to grow. This suggests that the enzyme was fully reduced by the substrate in the beginning and then slowly reoxidized either by a trace amount of oxygen present or by leakage in the system during the relatively long crystallization process. Fully grown crystals of the complex are golden yellow with an occasional orange or purplish tint, varying from crystal to crystal and batch to batch, compared to the bright clear yellow of the native crystals. This indicates that the enzyme flavin in the complex is a mixture of the fully reduced form, produced in the catalytic reaction, and semiquinone and oxidized forms produced by secondary oxidation. In addition, the enzyme flavin and the enoyl acyl ligand form charge-transfer complexes that yield a broad absorption band at long wavelengths (18). Since the initial amount of the substrate in the crystallization set-up was equimolar to the enzyme-bound flavin and the flavin appeared to be nearly completely reduced upon addition of the substrate, it is reasonable to assume that the fatty acyl ligand in the crystal is primarily the product, octenoyl-CoA. Kinetic investigation on pig kidney MCAD (19) has shown that various combinations of enzyme–ligand complexes exist: oxidized enzyme–substrate, reduced enzyme–product, and oxidized enzyme–product. Furthermore, the semiquinone forms of the enzyme could be stabilized by the acyl-CoA ligand in the crystal (20). Therefore, the complex between the enzyme and the acyl ligand in the crystal may be a mixture of all possible combinations of different oxidation states of the enzyme and the ligand. The exact proportions of the different enzyme species in each crystal could not be determined. In this report, we refer to the bound ligand as C_8-CoA, although the predominant form is probably octenoyl-CoA.

The two subunits in the asymmetric unit were treated independently at the final stages of the least-squares refinements for both the native and the complex structures. Analyses of a least-squares fit of the two crystallographically independent monomers yielded the rms deviations between the main-chain atoms and between all atoms of the two monomers. The rms values were 0.21 Å and 0.63 Å for the native and 0.19 Å and 0.46 Å for the complex, respectively. The two monomer structures are essentially identical within the error limits in both crystalline states.

The Polypeptide Fold and the Quaternary Structure. The overall polypeptide folding of the native MCAD has been described (12). The monomer is folded into three domains of approximately equal size (Fig. 1). The N-terminal and the C-terminal domains are mainly α-helices packed together and the middle domain consists of two orthogonal β-sheets. The FAD has an extended conformation. The flavin ring is buried in the crevice between the two α-helical domains and the β-sheet domain of one subunit, and the adenosine pyrophosphate moiety is stretched into the subunit junction with a neighboring subunit, composed of two C-terminal domains (Fig. 2). The polypeptide chain folding in both the native and the complex structures is essentially identical. The rms deviation for the main-chain atoms between the two structures is 0.26 Å, indicating that the overall chain folding of the polypeptide, as well as the quaternary structure, does not change with ligand binding. Fig. 2 shows an α-carbon tracing of a tetramer viewed along an axis $\approx 20°$ from a twofold axis. The molecule has 222 symmetry and is expected to have three distinct sets of intersubunit contacts along the three twofold axes between the red and green, red and purple, and red and blue subunits. The interactions between the red and the green subunits are along the noncrystallographic twofold axis and involve the FAD binding as well as the 3′-AMP moiety of the

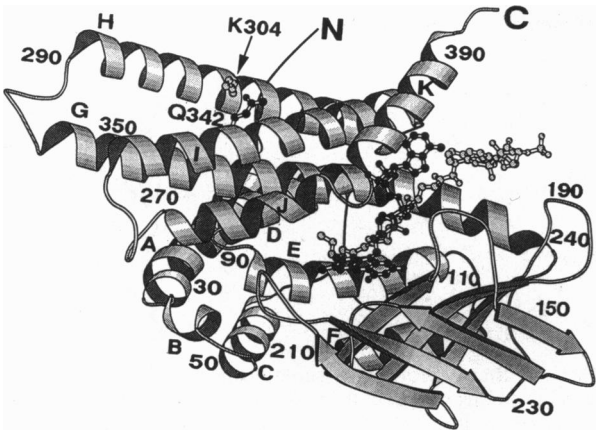

FIG. 1. Ribbon diagram of a monomer of the complex between MCAD and C_8-CoA. The overall polypeptide fold is the same as that of the native enzyme. N- and C-terminal ends are indicated and α-helices are lettered sequentially. Lys-304 and Gln-342 are represented with ball-and-stick models and are shown in the H- and I-helix, respectively. The FAD is represented by solid balls and the C_8-CoA is represented by open balls. The figure was drawn by using the program MOLSCRIPT (21).

substrate binding, suggesting that dimer formation is essential for enzyme activity. The tetramer is arranged as a dimer of dimers (northern and southern hemispheres) and the interactions between the dimers are mainly helix to helix on the equatorial plane. Both the N-terminal and the C-terminal ends of one dimer extend into the other dimer and lie on the surface of the molecule.

FAD–Polypeptide Interactions. The flavin ring is located in the crevice between the β-domain and the C-terminal domain of one subunit and the C-terminal domain of a neighboring subunit (Figs. 1 and 2). The pyrimidine portion of the isoalloxazine ring is surrounded by the residues from the loops between the β-strands and forms hydrogen bonds with polar side chains as well as with the main-chain atoms of the peptide. The dimethyl benzene portion of the ring is surrounded by the loop between the H- and G-helices of the neighboring subunit and its sinister (si) face is partially covered by Trp-166 and Met-165. The substrate associates with the rectus (re) face of the flavin, so ETF must interact with the dehydrogenase through the si side of the flavin, and Trp-166 and Met-165 might play a role in the transfer of the electrons between the two flavoproteins. There are many polar residues (Arg-210, Glu-212, Arg-223, Arg-164, and Glu-136) lying at the surface of the MCAD molecule around Trp-166 where ETF might bind the enzyme through electrostatic interactions (22). A detailed picture of the amino acid residues around the flavin ring and possible hydrogen bonds is shown in Fig. 3. There are no detectable differences between the hydrogen bonding schemes of the isoalloxazine ring in the free and C_8-CoA ligated structures. However, it is not clear from current studies whether the differences between the oxidized and the reduced states of flavin are so minor or whether the proportion of the reduced flavin is so small that the observed structure is essentially that of the oxidized flavin–product complex. The adenosine moiety of the FAD makes contacts with the other subunit of the dimer and lies at the surface of the tetrameric molecule. Arg-281 and Gly-353 of the neighboring subunit make hydrogen bonds with the oxygen atoms of the pyrophosphate, and Thr-263 and Gln-349 make hydrogen bonds with N7 of the adenine ring and 3′-hydroxyl group of the ribose, respectively.

The Active Site. A difference Fourier map ($F_{complex} - F_{nat}$) with phase angles from the refined native protein structure (excluding the water molecules) was calculated and averaged (17) about the noncrystallographic twofold axis. The resulting map showed tubular electron densities near the FAD ring and between the β-sheet domain and the two α-helix domains. Although a model of either octanoyl-CoA or octenoyl-CoA could be fitted to these densities, a *trans*-2-octenoyl-CoA model was used for the subsequent refinements. At the resolution of the present studies (2.4 Å), it cannot be distinguished unequivocally whether the bound ligand in the complexed structure is a substrate (saturated Cα—Cβ bond) or a product (Cα=Cβ double bond).

The overall shape of the enzyme-bound C_8-CoA molecule resembles the shape of the letter J; the 3′-AMP forms the short arm, the pyrophosphate the right angle turn, and the

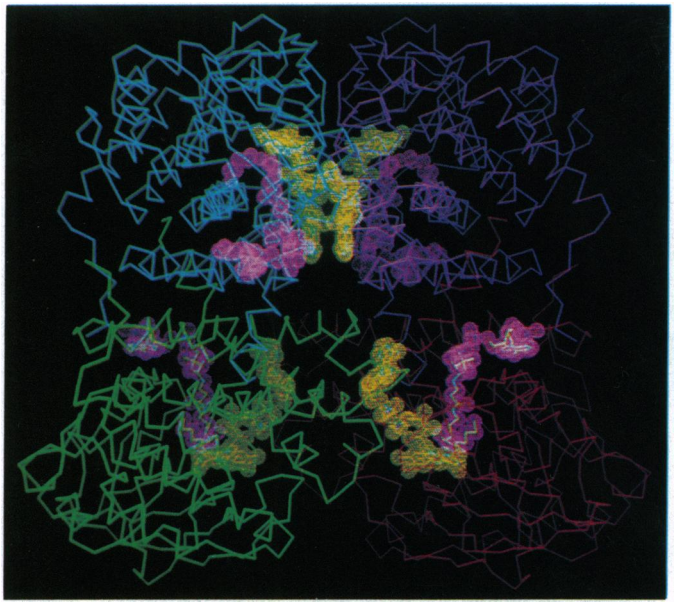

FIG. 2. Cα tracing of a tetramer of MCAD. The tetramer is viewed ≈20° away from a twofold axis. The red monomer is shown ≈45° rotated from the view seen in Fig. 1. The FAD and C_8-CoA are shown with van der Waal's surfaces in yellow and pink, respectively.

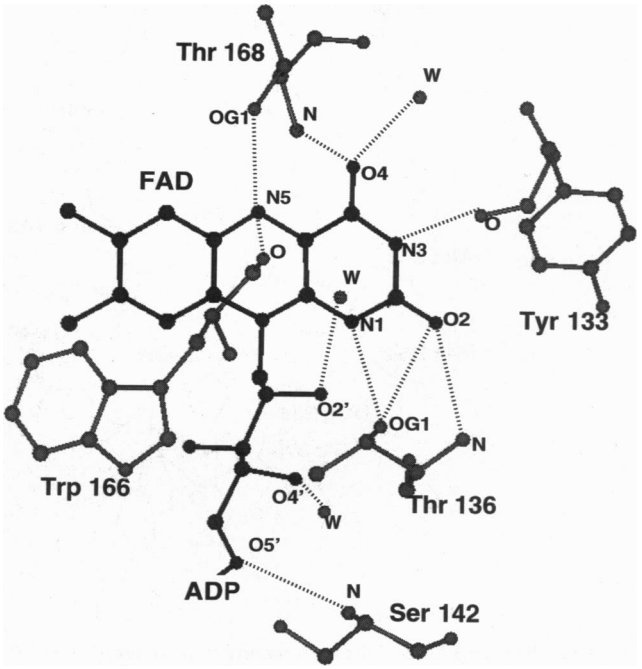

FIG. 3. Residues found near the FAD binding site. Potential hydrogen bonds between polar atoms <3.3 Å are shown as dashed lines. W, water molecule.

pantetheine moiety with the fatty acyl group are extended to form a long arm with a hook (Fig. 4). This conformation is similar to the acetyl-CoA structure observed in chloramphenicol acetyltransferase (23), whereas that found in citrate synthase is more compact (24). The alkyl chain of the acyl-CoA ligand in the MCAD structure is deeply buried inside of the protein, at the re side of the flavin, confirming the stereochemistry proposed by Pai and coworkers (25). The binding cavity for the fatty acyl moiety is located between helices E and G (Fig. 1) and is lined with the side chains of Glu-376, Tyr-375, Val-259, Thr-168, Leu-103, and Ala-100. Glu-99 and Thr-96 form the bottom of the deep hole where the end of the alkyl chain lies (Fig. 5). The C_α—C_β bond of the bound ligand molecule is sandwiched between the carboxylate of Glu-376 and the flavin ring, with distances 4.2–4.6 Å from the Cα to the carboxyl oxygens of Glu-376 and ≈3.3 Å between the C_β and N_5 of the FAD ring (Fig. 4). This arrangement is consistent with the α–β dehydrogenation mechanism proposed by Ghisla *et al.* (26). It also supports the proposal that Glu-376 is the base that abstracts the α proton of the acyl-CoA substrate (27). The carbonyl oxygen of the thioester is hydrogen bonded to ribityl 2′-hydroxyl group (2.9 Å) of the FAD as well as to the main-chain amide nitrogen of Glu-376 (3.1 Å). These interactions serve to lower the pK of the α proton of the substrate and also are responsible for the precise alignment of the flavin, substrate, and Glu-376 for the α,β-dehydrogenation reaction by anchoring the substrate at the appropriate depth and orientation into the deep hole of the active-site cavity. Preliminary results of studies with reconstituted enzymes with 2′- or 3′-deoxy-FAD confirmed the importance of the interaction between 2′-hydroxyl and the carbonyl oxygen of the substrate (28). The direct participation of the ribityl group of FAD in the activation of the substrate for the catalytic reaction has not been observed in other flavoenzymes that have been studied so far. The pantothenate and pyrophosphate portions of the substrate make no direct hydrogen bonds to the protein, and the 3′-AMP has only two potential hydrogen bonds (Fig. 4). The 3′-AMP end of the C_8-CoA is exposed to the solvent (Fig. 1).

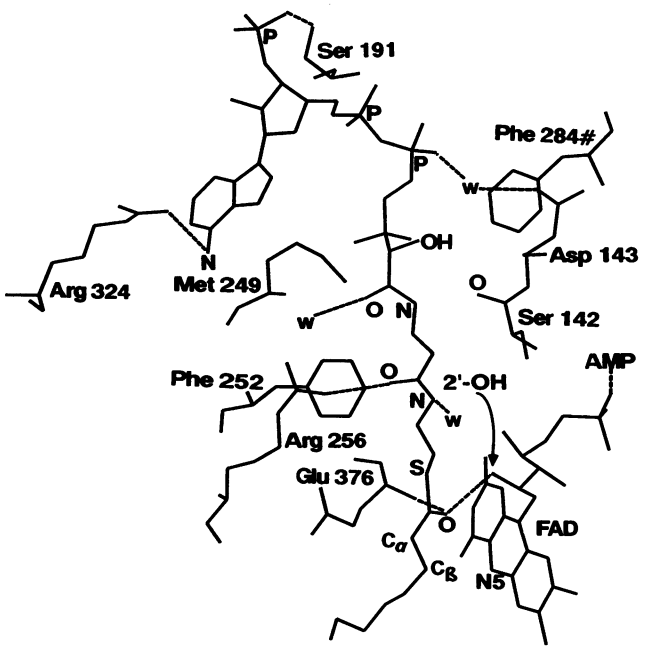

FIG. 4. Residues around the CoA moiety of the bound ligand. #, Residue numbers of the neighboring subunit of the dimer; W, ordered water molecules; dashed lines, hydrogen bonds. The carbonyl oxygen of the thioester is hydrogen bonded to both the ribityl 2′-hydroxyl group and the amide nitrogen of Glu-376.

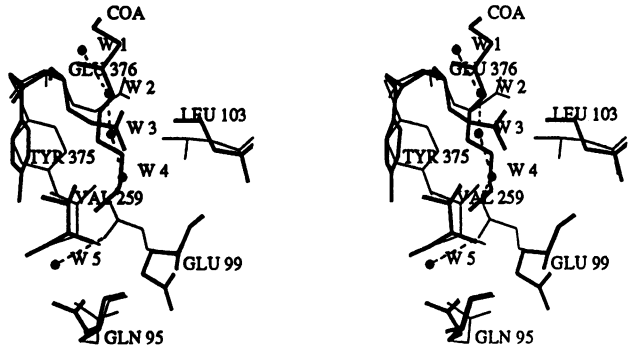

FIG. 5. Stereo drawing of superposition of the residues in the fatty acyl binding pocket of the native (thin lines) and the complexed enzyme (thick lines). For clarity, only residues with substantial differences in their conformations are shown. Tightly bound water molecules in the native structure are shown as solid spheres and labeled W. Hydrogen bonds are shown as dashed lines. Water W-4 is hydrogen bonded to one γ-carboxyl oxygen and water W-5 is bonded to the other carboxyl oxygen of Glu-99. The fatty acyl chain replaces the string of water molecules in the complex.

This is consistent with the results obtained by Frerman and his coworkers (29) in which 3′-dephospho-CoA and etheno-CoA analogues of octanoyl-CoA are almost as good substrates as octanoyl-CoA, whereas the compounds that differ in the fatty acyl moiety such as free CoA, acetyl-CoA, or propionyl-CoA are very poor inhibitors (29). The binding mode of the CoA moiety to the enzyme is somewhat similar to those observed in citrate synthase (24) and in chloramphenicol acetyltransferase (23) in that the pantetheine portion of the molecule is shielded from the bulk solvent, whereas the phosphates lie at the surface of the molecule. The "adenine binding loop" described in the structure of citrate synthase is not observed in MCAD.

Although the main-chain conformation and the quaternary structure are unchanged upon complex formation, many differences are observed in the side-chain conformations of the residues, particularly at the active site (Fig. 5). The carboxylate of Glu-376 swings toward the C_α atom of the substrate, ready to abstract its proton. Tyr-375 is conserved in all acyl-CoA dehydrogenases sequenced (30) and the plane of the phenolic side chain is tilted to face rather than to be edge on to the alkyl chain of the substrate. The most pronounced side-chain movement upon binding of the ligand is that of Glu-99, which turns almost 90° making the substrate binding "hole" deeper. Side chains of Leu-103, Val-259, and Gln-95, which surround the alkyl chain, move away from the bound ligand to make more room. In the native enzyme structure, the active site cavity is filled with a string of well-ordered water molecules (Fig. 5). The ribityl 2′-hydroxyl group of FAD is hydrogen bonded to water W-1; waters W-1, W-2, W-3, and W-4, carboxylate oxygens of Glu-99, and water W-5 are connected in series via hydrogen bonds. In the complexed enzyme structure, the string of water beads is broken and W-1 through W-4 are replaced by the fatty acyl thioester moiety of the ligand. The positioning of the ligand is such that the carbonyl oxygen of the thioester occupies roughly the same position that W-1 does in the native structure, Glu-99 moves away to make enough room for the tail end of the fatty acyl chain, and W-5 remains and bonds tightly to the hydroxyl groups of Tyr-372, Tyr-375, and the γ-amide group of Gln-95. In the complexed structure, there are no ordered water molecules in the vicinity of the C_α—C_β bond of the ligand nor is there any room for solvent water molecules or molecular oxygen to be accommodated. It has been observed that substrate and certain substrate analogues of acyl-CoA dehydrogenases markedly reduce the rate of reoxidation of the reduced enzyme by molecular oxygen (31).

The tight binding of the fatty acyl chain in the active site hole is likely to prevent molecular oxygen from approaching the flavin ring. The displacement of water molecules in the fatty acyl cavity upon substrate binding is in agreement with the hypothesis of Wang and Thorpe (32) who proposed that the protection of the reduced enzyme from molecular oxygen is due to the desolvation of the active site and consequent destabilization of the superoxide anion formed during reoxidation of flavin. Since thioethers give 10^{-2} to 10^{-3} times the protection of thioesters, it would be interesting to see whether any water molecule, particularly W-1, remains in the active site when thioether analogues bind to the enzyme. It is tempting to speculate that some of the water "beads" serve as nucleophiles in the intrinsic hydratase activity of MCAD that is observed with substrates shorter than C_8-CoA (33).

Lys-304 Is Not in the Vicinity of the Active Site. The prevalent mutation found in patients with MCAD deficiency is a point mutation, A → G, at nt 985 in the MCAD gene, which results in the Lys-304 → Glu substitution (34–36). Lys-304 is located in the middle of the H-helix, forming a hydrogen bond with the γ-carbonyl oxygen of Gln-342 that lies in the I-helix (Fig. 1). It lies ≈20 Å away from the active site and is not involved in binding of the substrate or FAD. Glu-304 in the mutant protein is also capable of forming a hydrogen bond with the γ-amido-NH_2 of Gln-342. There are two other acidic residues, Asp-300 and Asp-346, within 6 Å of the γ-carboxylate of Glu-304. Furthermore, these residues lie at the dimer–dimer interface of the tetramer. This concentration of negative charge could affect the polypeptide folding and the tetramer formation and result in instability of the enzyme.

We thank A. W. Strauss for providing us amino acid sequence data of pig MCAD and F. E. Frerman for helpful discussions. We also thank S. Ghisla for drawing our attention to the interactions between the ribityl chain of the FAD and the substrate, and N. H. Xoung and his group for assistance in data collection at the Resource for Protein Crystallography at the University of California-San Diego. Some of the computations were carried out at the Pittsburgh Supercomputer Center. This research is supported by grants from the National Institutes of Health (GM29076) and from the National Science Foundation (DIR-8722022).

1. Crane, F. L., Mil, S., Hauge, J. G., Green, D. E. & Beinert, H. (1956) *J. Biol. Chem.* **218**, 701–716.
2. Crane, F. L. & Beinert, H. (1956) *J. Biol. Chem.* **218**, 717–731.
3. Ruzicka, F. J. & Beinert, H. (1977) *J. Biol. Chem.* **252**, 8440–8445.
4. Beinert, H. (1963) in *The Enzymes*, eds. Boyer, P. D., Lardy, H. & Myrback, K. (Academic, New York), Vol. 7, pp. 447–473.
5. Izai, K., Uchida, Y., Ori, T., Yamamoto, S. & Hashimoto, T. (1992) *J. Biol. Chem.* **267**, 1027–1033.
6. Ikeda, Y. & Tanaka, K. (1983) *J. Biol. Chem.* **258**, 1077–1085.
7. Ikeda, Y. & Tanaka, K. (1983) *J. Biol. Chem.* **258**, 9477–9487.
8. Lenich, A. C. & Goodman, S. I. (1986) *J. Biol. Chem.* **261**, 4090–4096.
9. Stanley, C. A., Hale, D. E. & Coates, P. M. (1990) in *Fatty Acid Oxidation: Clinical, Biochemical and Molecular Aspects*, eds. Tanaka, K. & Coates, P. M. (Liss, New York), pp. 291–302.
10. Roe, C. R. & Coates, P. M. (1989) in *The Metabolic Basis of Inherited Disease*, eds. Scriver, C. R., Beaudet, A. L., Sly, W. S. & Valle, D. (McGraw–Hill, New York), 6th ed., Vol. 1, pp. 889–914.
11. Kelly, D. P., Kim, J.-J. P., Billadello, J. J., Hainline, B. E., Chu, T. W. & Strauss, A. W. (1987) *Proc. Natl. Acad. Sci. USA* **84**, 4068–4072.
12. Kim, J.-J. P. & Wu, J. (1988) *Proc. Natl. Acad. Sci. USA* **85**, 6677–6681.
13. Kim, J.-J. P., Wang, M., Djordjevic, S. & Paschke, R. (1992) in *New Developments in Fatty Acid Oxidation*, eds. Coates, P. M. & Tanaka, K. (Wiley–Liss, New York), pp. 111–126.
14. Cambillau, C. & Horjales, E. (1987) *J. Mol. Graph.* **5**, 174–177.
15. Brünger, A. T., Kuriyan, J. & Karplus, M. (1987) *Science* **235**, 458–460.
16. Hendrickson, W. A. & Konnert, J. H. (1980) in *Biomolecular Structure, Function, Conformation and Evolution*, ed. Srinivasan, R. (Pergamon, Oxford), Vol. 1, pp. 43–75.
17. Bricogne, C. T. (1976) *Acta Crystallogr. Sect. A* **32**, 832–837.
18. Massey, V. & Ghisla, S. (1974) *Ann. N.Y. Acad. Sci.* **227**, 446–465.
19. Schopfer, L. M., Massey, V., Ghisla, S. & Thorpe, C. (1988) *Biochemistry* **27**, 6599–6611.
20. Mizzer, J. P. & Thorpe, C. (1981) *Biochemistry* **20**, 4965–4970.
21. Kraulis, P. J. (1991) *J. Appl. Crystallogr.* **24**, 946–950.
22. Beckman, J. D. & Frerman, F. E. (1983) *J. Biol. Chem.* **258**, 7563–7569.
23. Leslie, A. G. W., Moody, P. C. E. & Shaw, W. V. (1988) *Proc. Natl. Acad. Sci. USA* **85**, 4133–4137.
24. Remington, S., Wiegand, G. & Huber, R. (1982) *J. Mol. Biol.* **158**, 111–152.
25. Manstein, D. J., Pai, E. F., Schopfer, L. M. & Massey, V. (1986) *Biochemistry* **25**, 6807–6816.
26. Ghisla, S., Thorpe, C. D. & Massey, V. (1984) *Biochemistry* **23**, 3154–3161.
27. Powell, P. J. & Thorpe, C. (1988) *Biochemistry* **27**, 8022–8028.
28. Ghisla, S., Engst, S., Moll, M., Bross, P., Strauss, A. W. & Kim, J.-J. P. (1992) in *New Developments in Fatty Acid Oxidation*, eds. Coates, P. M. & Tanaka, K. (Wiley–Liss, New York), pp. 127–142.
29. Frerman, F. E., Miziorko, H. M. & Beckman, J. D. (1980) *J. Biol. Chem.* **255**, 11192–11198.
30. Matsubara, Y., Indo, Y., Naito, E., Ozasa, H., Glassberg, R., Vockley, J., Ikeda, Y., Kraus, J. & Tanaka, K. (1989) *J. Biol. Chem.* **264**, 16321–16331.
31. Beinert, H. & Page, E. (1957) *J. Biol. Chem.* **225**, 479–497.
32. Wang, R. & Thorpe, C. (1991) *Biochemistry* **30**, 7895–7901.
33. Lau, S.-M., Powell, P., Buettner, H., Ghisla, S. & Thorpe, C. (1986) *Biochemistry* **25**, 4184–4189.
34. Matsubara, V., Narisawa, K., Miyabayashi, S., Tada, K. & Coates, P. M. (1990) *Lancet* **335**, 1589.
35. Yokota, I., Indo, Y., Coates, P. M. & Tanaka, K. (1990) *J. Clin. Invest.* **86**, 1000–1003.
36. Kelly, D. P., Whelan, A. J., Ogden, M. L., Alpers, R., Zang, Z., Bellus, G., Gregersen, N., Dorland, L. & Strauss, A. (1990) *Proc. Natl. Acad. Sci. USA* **87**, 9236–9240.